ISSCR

Defining the Role of Oxygen Tension in Human Neural Progenitor Fate

Yuan Xie,[1,2] Jin Zhang,[3] Ying Lin,[1] Xavier Gaeta,[1] Xiangzhi Meng,[1] Dona R.R. Wisidagama,[4] Jessica Cinkornpumin,[1,2] Carla M. Koehler,[5,6] Cindy S. Malone,[4] Michael A. Teitell,[2,3,6,7,8,*] and William E. Lowry[1,2,6,7,*]

[1]Department of Molecular Cell and Developmental Biology, University of California, Los Angeles, Los Angeles, CA 90095, USA
[2]Eli and Edythe Center for Regenerative Medicine and Stem Cell Research, University of California, Los Angeles, Los Angeles, CA 90095, USA
[3]Department of Pathology and Laboratory Medicine, University of California, Los Angeles, Los Angeles, CA 90095, USA
[4]Department of Biology, California State University, Northridge, Northridge, CA 91330, USA
[5]Department of Chemistry and Biochemistry, University of California, Los Angeles, Los Angeles, CA 90095, USA
[6]Molecular Biology Institute, University of California, Los Angeles, Los Angeles, CA 90095, USA
[7]Jonsson Comprehensive Cancer Center, University of California, Los Angeles, Los Angeles, CA 90095, USA
[8]California NanoSystems Institute, University of California, Los Angeles, Los Angeles, CA 90095, USA
*Correspondence: mteitell@ucla.edu (M.A.T.), blowry@ucla.edu (W.E.L.)
http://dx.doi.org/10.1016/j.stemcr.2014.09.021

SUMMARY

Hypoxia augments human embryonic stem cell (hESC) self-renewal via hypoxia-inducible factor 2α-activated *OCT4* transcription. Hypoxia also increases the efficiency of reprogramming differentiated cells to a pluripotent-like state. Combined, these findings suggest that low O_2 tension would impair the purposeful differentiation of pluripotent stem cells. Here, we show that low O_2 tension and hypoxia-inducible factor (HIF) activity instead promote appropriate hESC differentiation. Through gain- and loss-of-function studies, we implicate O_2 tension as a modifier of a key cell fate decision, namely whether neural progenitors differentiate toward neurons or glia. Furthermore, our data show that even transient changes in O_2 concentration can affect cell fate through HIF by regulating the activity of MYC, a regulator of LIN28/*let-7* that is critical for fate decisions in the neural lineage. We also identify key small molecules that can take advantage of this pathway to quickly and efficiently promote the development of mature cell types.

INTRODUCTION

Human embryonic stem cells (hESCs) originate from the blastocyst inner cell mass (Thomson et al., 1998), which is in a hypoxic microenvironment estimated at 1.5%–5.3% O_2 in the mammalian reproductive tract (Dunwoodie, 2009; Mohyeldin et al., 2010; Simon and Keith, 2008). hESCs grown in physiological O_2 (∼5% or less O_2) self-renew with reduced levels of spontaneous differentiation compared with hESCs grown in atmospheric O_2 (∼21% O_2) (Ezashi et al., 2005; Westfall et al., 2008). hESCs isolated and passed exclusively in physiological O_2 contain two active X chromosomes (XaXa), marking a less differentiated state than that in atmospheric O_2, which typically contains one inactive X chromosome (Lengner et al., 2010). Physiological O_2 also improves the efficiency of defined factor-induced cellular reprogramming to a pluripotent-like state (Yoshida et al., 2009). Combined, these studies show the importance of physiological O_2 in supporting stem cell self-renewal and in suppressing spontaneous, usually unwanted hESC differentiation.

Studies on the role of O_2 tension in promoting pluripotency have indicated hypoxia-inducible factor 2α (HIF2α) (also called endothelial PAS domain protein 1) and HIF3α in the transcriptional upregulation of *OCT4* in hESCs (Forristal et al., 2010). These findings are also consistent with

the role of HIF2α in transactivating *Oct4* expression in mouse ESCs (Covello et al., 2006). Since the activation of HIF pathway appears to favor self-renewal, it might be expected that HIF activity would also inhibit purposeful hESC differentiation. Four studies have examined the effects of hypoxia on early hESC differentiation, but none has specifically examined the role of HIF. In these studies, hESCs in physiological O_2 showed enhanced embryoid body (EB) formation or endothelial and cardiomyocyte differentiation (Ezashi et al., 2005; Lim et al., 2011; Ng et al., 2010; Prado-Lopez et al., 2010). However, physiological O_2 induces pleiotropic cellular and molecular effects, and the underlying cause(s) for paradoxically enhanced EB or lineage formation in physiological O_2 is unclear. For example, the O_2 concentration is known to affect (1) oxidative stress and hESC growth (Ezashi et al., 2005); (2) the activity of O_2-dependent enzymes, such as Jumonji domain-containing dioxygenases (Xia et al., 2009), which have broad roles in the epigenetic regulation of gene expression; (3) multiple O_2-sensing signal transduction pathways, including the mechanistic target of rapamycin (mTOR) pathway (Wouters and Koritzinsky, 2008) and the unfolded protein response-activated endoplasmic reticulum stress pathway (Wouters and Koritzinsky, 2008); and (4) the HIF-controlled gene transcription network (Lendahl et al., 2009). Therefore, it remains unclear whether the enhancement of EB or lineage specific differentiation in

Figure 1. Germ Layer Formation Is Regulated by the Oxygen Sensing Pathway

(A) Embryoid bodies cultured in physiological (2% O_2) or atmospheric oxygen (20% O_2) concentrations display markedly different gene expression profiles, with the Venn diagram outlining the number of genes different. GO analysis suggested that acquisition of all three germ layers was affected by oxygen concentration. All genes in the Venn diagram were induced over 5-fold in EBs relative to undifferentiated PSCs.

(legend continued on next page)

physiological O_2 occurs mainly through HIF transactivation or other molecular mechanisms.

HIFs are major regulators of the cellular response to O_2 tension (Denko, 2008; Lendahl et al., 2009; Majmundar et al., 2010). HIFs form a heterodimer composed of HIFα and HIF1β (also called aryl hydrocarbon receptor nuclear translocator) to transactivate hypoxia-responsive genes. They are regulated at the level of α-subunit protein stability in an O_2-dependent manner. When oxygen is abundant, HIFα subunits are hydroxylated by prolyl hydroxylase domain (PHD) proteins (in the presence of Fe^{2+}) and recognized by an E3 ubiquitin ligase, VHL (Von Hippel-Lindau), leading to degradation in the proteasome. In hypoxic conditions, decreased O_2 diminishes enzymatic activity of PHDs. As a result, HIF1α and HIF2α proteins are stabilized and dimerize with HIF1β in the nucleus to transactivate specific target genes. In *Hif1α*, *Hif2α*, and *Hif1β* knockout mice, deficient HIF activity impaired placental development (Adelman et al., 2000; Cowden Dahl et al., 2005; Kozak et al., 1997), heart development (Krishnan et al., 2008; Licht et al., 2006), and endochondrial bone formation during early embryogenesis (Amarilio et al., 2007; Dunwoodie, 2009; Provot et al., 2007). Furthermore, conditional knockout mice of *Hif1α* in the central nervous system exhibit hydrocephalus accompanied by a reduction in neural cells and an impairment of spatial memory (Tomita et al., 2003). Those studies demonstrated the importance of *Hifs* in normal brain development. It is clear from the vast majority of studies on human pluripotent cell differentiation that typical protocols generate cells more akin to those found during the earliest stages of tissue formation, prior to significant tissue vascularization. What is less understood is whether methods to culture cells that more accurately replicate in vivo conditions can affect the developmental potential of pluripotent progeny.

Previous studies describing antagonism between HIF and v-Myc avian myelocytomatosis viral oncogene homolog (MYC) were mostly in the context of cancer, and the roles of HIF1α and HIF2α were determined to be distinct. HIF1α induced cell cycle arrest by functionally counteracting MYC through p21^{cip1} (Koshiji et al., 2004). HIF1α induced MXI1 expression to inhibit a subset of MYC target genes that are involved in mitochondrial biogenesis and oxygen consumption (Corn et al., 2005; Zhang et al., 2007). However, HIF2α promoted cell proliferation in various cell lines under hypoxic conditions by stimulating MYC binding to its target gene promoters (Gordan et al., 2007). Increased HIF2α and decreased p21 level in patients with VHL gene mutations could lead to increased hepatocyte proliferation, which explained the increased volumes of liver relative to their body mass (Yoon et al., 2010). Most of the studies mentioned above were performed in disease models and thus may not be applicable to normal human development.

To determine whether O_2 tension regulates differentiation from pluripotent stem cells (PSCs) and affects the developmental maturity of their progeny, we specifically evaluated HIF transactivation in both undirected and directed hESC differentiation using loss- and gain-of-function approaches. We report that HIF activity is required for induction of appropriate germ layer specification. In addition, we identify LIN28 and *let-7* family microRNAs as key molecular nodes through which HIF activity promotes appropriate directed differentiation of neural progenitors toward either neurons or glia through MYC. Our study reveals that O_2 tension and HIF activity could be vital to maintaining appropriate fate progression in vitro and identify simple methods to facilitate these transitions.

RESULTS

Oxygen Tension Regulates Human Germ Layer Formation

Using EB formation from human PSCs as a model of germ layer formation, we assayed the role of O_2 tension by altering the concentration of O_2 in culture. As shown in Figure 1, reducing the O_2 tension to levels more close to physiological conditions (2% O_2) dramatically altered the acquisition of germ layer fates in EBs, as measured by transcriptome profiling (Figure 1A) for hallmark genes. Gene ontology (GO) analysis demonstrated that neural, vascular, and skeletal differentiation was altered by changes in O_2 concentration (Figure 1A). In particular, neural differentiation appeared to be significantly promoted in EBs generated in physiological O_2 at the expense of other lineages,
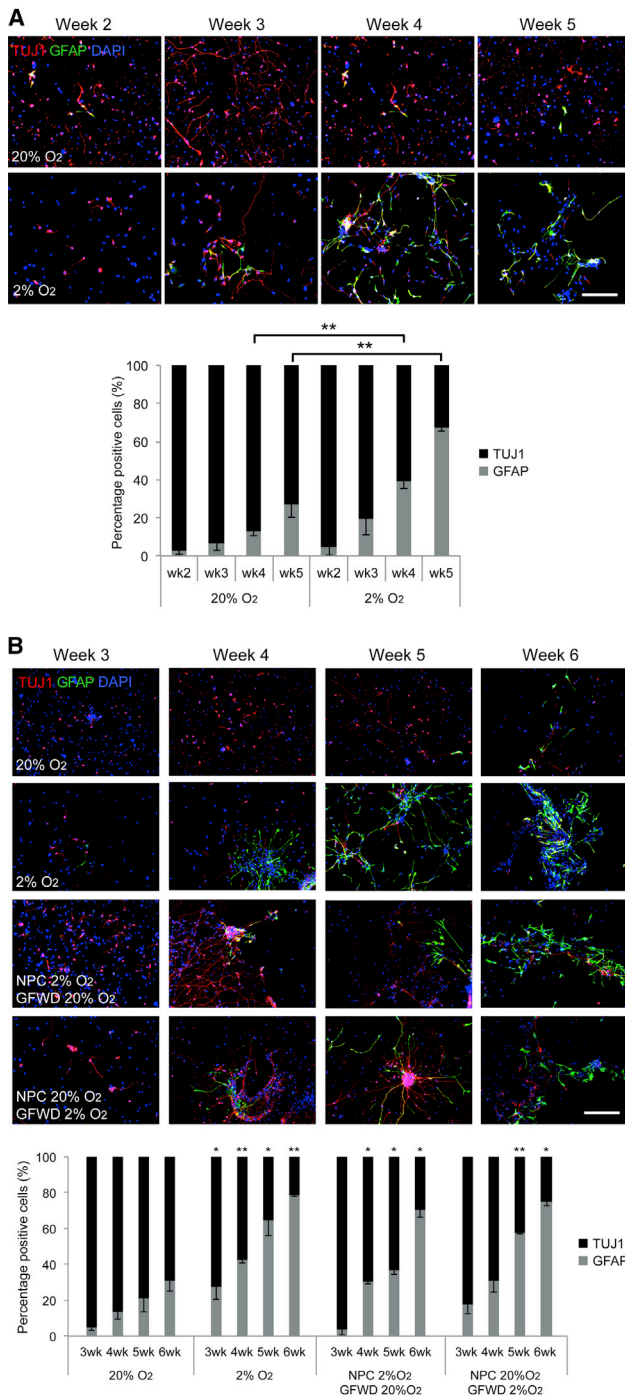
(B) Genes involved in neural differentiation are more dramatically induced in EBs grown in physiological oxygen concentration than EBs grown in atmospheric oxygen concentration. All genes listed here were induced over 5-fold in EBs relative to undifferentiated PSCs.

(C) hESCs with stable introduction of shRNA against HIF1β were used to make EBs under physiological oxygen concentration. Germ layer formation was measured by gene expression profiling and found to be affected as indicated by the Venn diagram. GO analysis uncovered the neuron, heart, and skeletal systems profoundly affected.

(D) A list of genes and the relative fold change for each in EBs relative to undifferentiated PSCs in either the presence or absence of normal HIF signaling.

(E) A Venn diagram of genes induced in 20% O_2, 2% O_2, and shHIF1β EBs.

See also Figure S1.

with classic markers such as *SOX1*, *HES5*, *FOXG1*, and other neural lineage genes all induced (Figure 1B).

Since O_2 levels are monitored molecularly by the HIF pathway (Figure S1 available online), we blocked HIF1α or HIF1β using small hairpin RNA (shRNA) (Figure S1). Generating EBs with stable knockdown of either HIF1α or HIF1β under physiological O_2 conditions disrupted gene expression significantly (Figure 1C) and altered the acquisition of neural, cardiac, and skeletal muscle lineages (Figure 1D). Many of the gene expression changes induced by altering the HIF sensing machinery were also validated in independent EB experiments by RT-PCR (Figure S1F). As anticipated, the genes changed by altering O_2 levels were highly similar to those affected by shHIF1β (Figure 1E), demonstrating the critical role for HIF1β in O_2 sensing during EB formation. These data demonstrate that the HIF O_2 sensing pathway regulates appropriate early undirected differentiation and potentially germ layer acquisition. To determine whether the HIF pathway is also important for directed differentiation, PSCs were subjected to culture conditions that promote the neural lineage.

Developmental Maturity of the Neural Lineage Is Regulated by Oxygen Tension

Human PSCs can be driven toward the neural lineage by simply changing the culture medium and generating rosette structures. Rosette-derived neural progenitor cells (NPCs) can generate both neurons and glia. Human PSC-derived NPCs typically differentiate into neurons with a small proportion of glia. Current consensus suggests that this neuronal bias is due to the developmental immaturity of pluripotent derivatives and the fact that neurogenesis precedes gliogenesis during development (Miyata et al., 2010). Most of the experiments that have generated this consensus have thus far been carried out in atmospheric O_2; therefore, we assayed the effect of lowering the O_2 tension in human NPC cultures. Remarkably, simply lowering the concentration of O_2 in NPC cultures completely shifted the bias away from neuronal toward glia differentiation (Figures 2A and S2B), suggesting that O_2 tension can affect cell fate decisions in the neural lineage. Interestingly, even just a brief exposure of NPCs to a physiological O_2

Figure 2. Neurogenesis Is Affected by Oxygen Tension
(A) Directed differentiation of NPCs toward neurons and glia by GFWD for 2–5 weeks assays for developmental maturity of progenitors (top). Culturing NPCs in either physiological or atmospheric oxygen concentration followed by growth factor withdrawal (GFWD) for the indicated times generates both neurons and glia, which are assayed by immunostaining for TUJ1 (neurons) or GFAP (glia). Quantification of immunostaining demonstrates the strong effect of physiological oxygen on gliogenesis (bottom).

(B) GFWD assay with NPCs grown in different conditions to assess the permanence of the effect of physiological oxygen on differentiation. NPCs were either grown under physiological or atmospheric oxygen for 5 days and then maintained under such conditions or switched to lower/higher oxygen during GFWD. Quantification shows that even a brief exposure to physiological oxygen drives gliogenesis (n = 3 independent experiments; mean ± SEM; *p < 0.05, **p < 0.01; Student's t test compared with 20% O_2 at each time point; scale bars, 200 μm).
See also Figure S2.
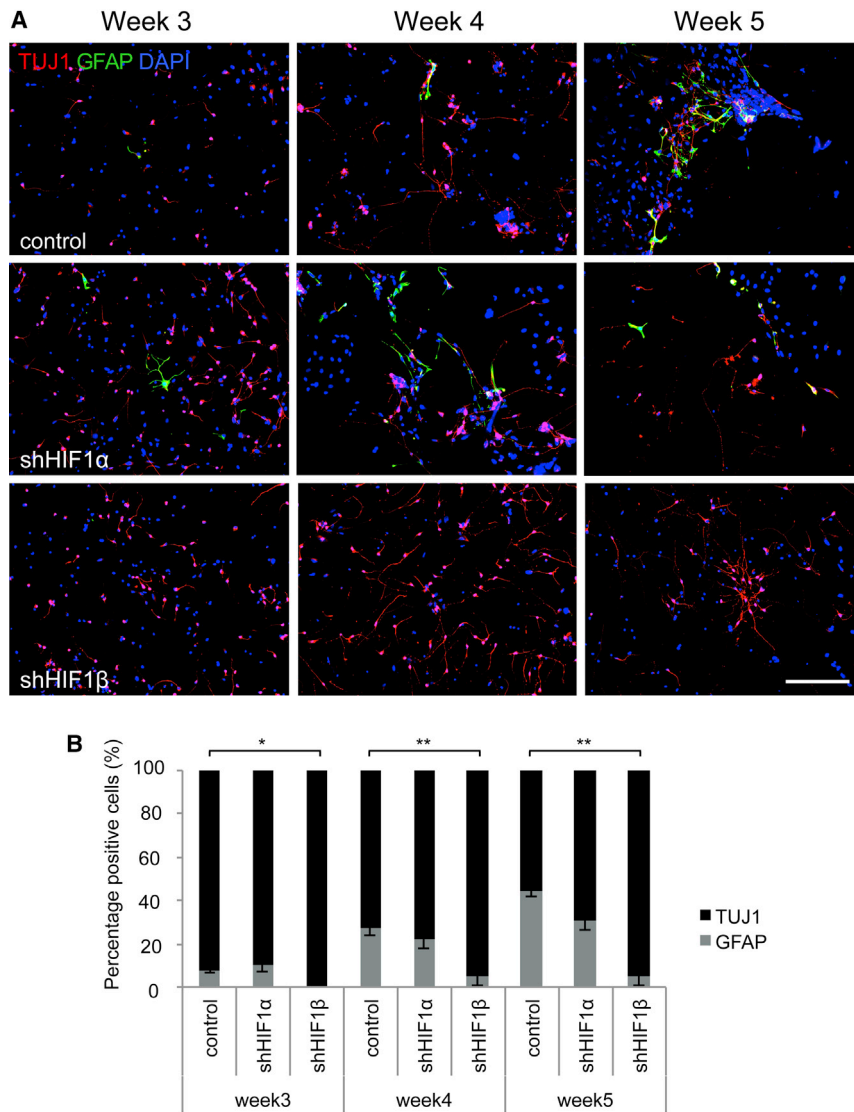
Figure 3. The HIF Pathway Regulates Neurogenesis

(A) NPCs were generated from hESC lines with stable integration of shRNA against HIF1α, HIF1β, or scramble control.

(B) GFWD assay and quantification of neurons (TUJ1) and glia (GFAP) indicate that HIF1β is required for gliogenesis in physiological oxygen concentration (n = 3 independent experiments; mean ± SEM; *p < 0.05, **p < 0.01; Student's t test compared with control at each time point; scale bars, 200 μm).

concentration influenced cell fate in the neural lineage toward glial production (Figure 2B), suggesting that the O_2 sensing machinery induces a lasting effect on NPC differentiation potential. Cell cycle analysis suggested that the effect of low O_2 tension on differentiation was not related to cell cycle changes (Figure S2A). Furthermore, immunostaining of NPCs in 2% and 20% O_2 suggested that the glial induction was not due to changes of apoptosis as the percentage of cells positive for cleaved caspase 3 was less than 1.5% in all conditions tested (Figure S2C).

To delineate the role of the O_2 sensing pathway in neural fate decisions, the shHIF1α and shHIF1β hESC lines were used to make NPCs. Relative to control lines, NPCs with reduced HIF signaling displayed an almost complete block in producing astroglia in 2% O_2 (Figures 3A and 3B), consistent with our data showing that HIF stabilization in physi-

ologic O_2 drives gliogenesis. Note that HIF1β knockdown had a more significant role in blocking gliogenesis than knocking down HIF1α. Because HIF1β forms heterodimer with either HIF1α or HIF2α, we tested the role of HIF2α in this cell fate decision. Despite the fact that some reports argue for differential roles for HIF1α versus HIF2α, we found that silencing HIF2α either by siRNA or by shRNA blocked the effect of low oxygen on gliogenesis in PSC-NPCs (Figures S3C and S3D). These results demonstrate that O_2 concentration is a key mediator of neurogenesis through the HIF signaling pathway.

Furthermore, several small molecules have been identified that induce the HIF pathway by blocking HIF degradation. Deferoxamine (DFX) stabilizes HIF by chelating Fe^{2+}, which is required for enzymatic activity of PHDs. NPCs grown in atmospheric O_2 and treated with DFX showed a
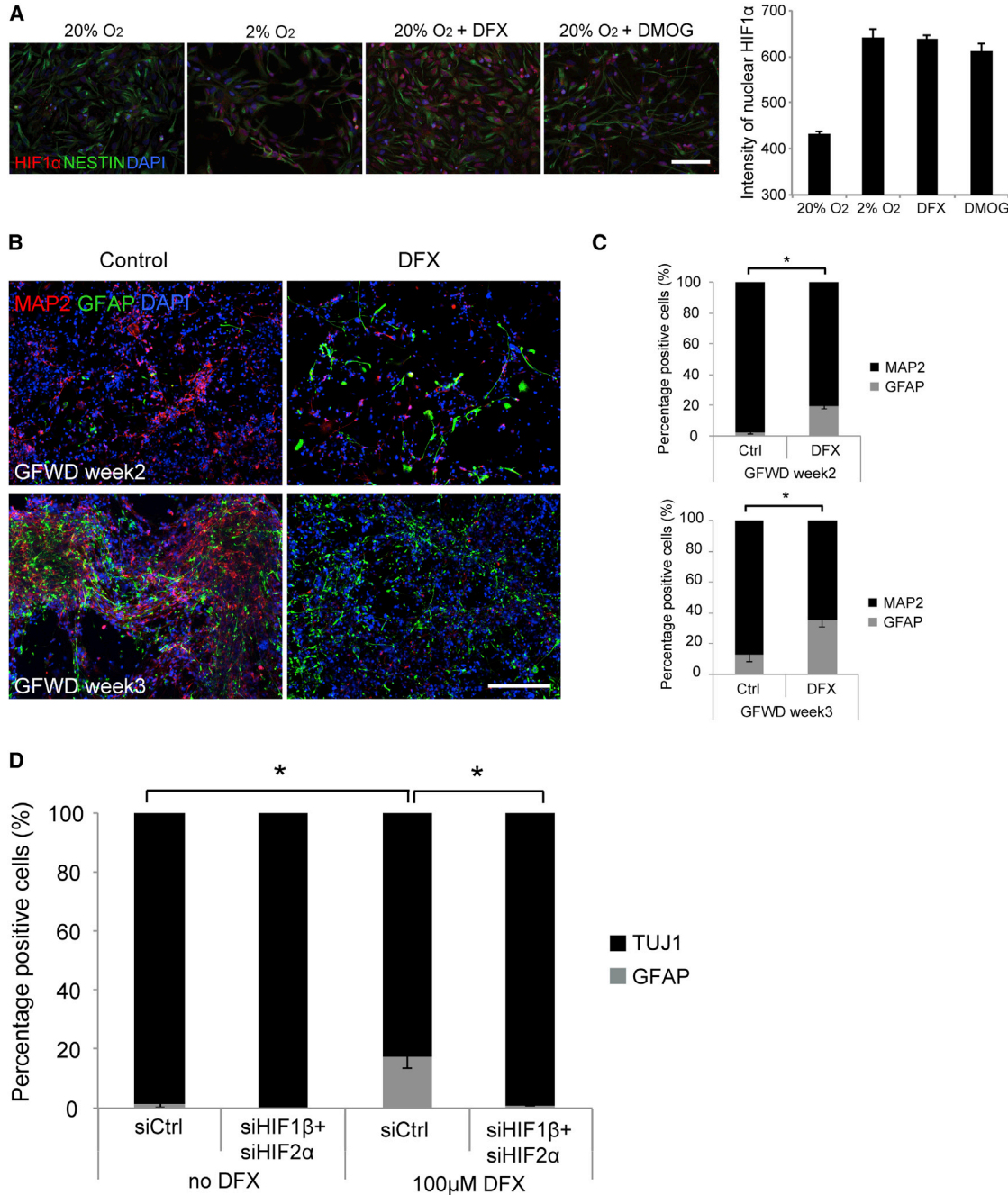
Figure 4. Small Molecule-Driven HIF Activation Can Drive Gliogenesis

(A) Immunostaining for HIF1α proteins in the nucleus showed that lowering oxygen to 2% was sufficient to drive nuclear translocation and stabilization of HIF1α. Using small molecule inhibitors of HIF degradation (DFX and dimethyloxalylglycine [DMOG]) also led to HIF1α stabilization and nuclear localization, even in the presence of 20% oxygen (n > 100 cells per treatment; mean ± SEM; scale bars, 100 μm).

(B) In GFWD assays, DFX treatment led to an increase in astrocytes as measured by GFAP at different time points.

(C) A quantification of percentage of neurons (MAP2) and astrocytes (GFAP) at indicated time points (n = 3 independent experiments with two different human ESC-derived NPCs and one human iPSC-derived NPC; mean ± SEM; *p < 0.05; Student's t test; scale bars, 200 μm).

(D) GFWD assay with siRNA against HIF1β and HIF2α demonstrated that the effect of DFX on gliogenesis strictly depends on the HIF sensing pathway (n = 3 independent experiments; mean ± SEM; *p < 0.05; Student's t test).

See also Figure S3.

translocation of HIF1α to the nucleus (Figure 4A) and a distinct increase in gliogenesis, as shown for NPCs grown in physiological O_2 (Figures 4B and 4C). Importantly, key HIF target genes were induced by these manipulations, demonstrating bona fide HIF activation, such as *VEGFA*, *HK1*, *HK2*, *PGK1*, *PDK1*, and *HIF2α* (Figures S3A and S3B). Because silencing HIF1β and HIF2α each had significant effects on gliogenesis, we tested the effect of DFX when both of these key HIF transducers were silenced. In fact, gliogenesis was not affected in cells lacking these key mediators of the O_2-sensing pathway (Figure 4D), demonstrating that DFX indeed acts through the HIF pathway. Combined, these data show that HIF pathway signaling has an influence on cell fate decisions within the nervous system and also provides a rather simple method to create NPCs with a glial differentiation bias.

Molecular Mechanism of Neurogenesis by the HIF Pathway

To understand how the HIF pathway can regulate NPC fate decisions, we probed for the gene expression changes induced by altering HIF activity with various methods. As shown above, HIF activity and neurogenesis were influenced by stabilizing HIF with DFX or removal of HIF1β. We also overlaid differentially expressed genes between PSC-derived NPCs and human fetal brain-derived NPCs, which are highly gliogenic and more developmentally mature than PSC-NPCs (Patterson et al., 2012). Just a few gene expression changes were in common for all the manipulations performed, including *LIN28A* (Figure 5A), a gene previously implicated in neurogenesis (Balzer et al., 2010; Cimadamore et al., 2013; Kawahara et al., 2011). To gain mechanistic insight into the function of HIF, we evaluated a broader profile of gene expression changes and attempted to identify common regulatory elements in those genes affected changes in HIF activity. Gene Set Enrichment Analysis (GSEA) identified a number of regulatory elements among the group of genes affected by changes in HIF activity (Table S1). At the top of the list was HIF and MYC, suggesting that a large number of genes affected by HIF activity are potentially MYC target genes (Figure 5B). Narrowing gene expression changes to those genes known to be directly regulated by HIF showed almost universal induction of HIF target genes (Figure 5C). On the other hand, a similar analysis of MYC targets showed that roughly half of these genes were induced by physiological O_2, whereas the other half of these genes was suppressed (Figure 5D).
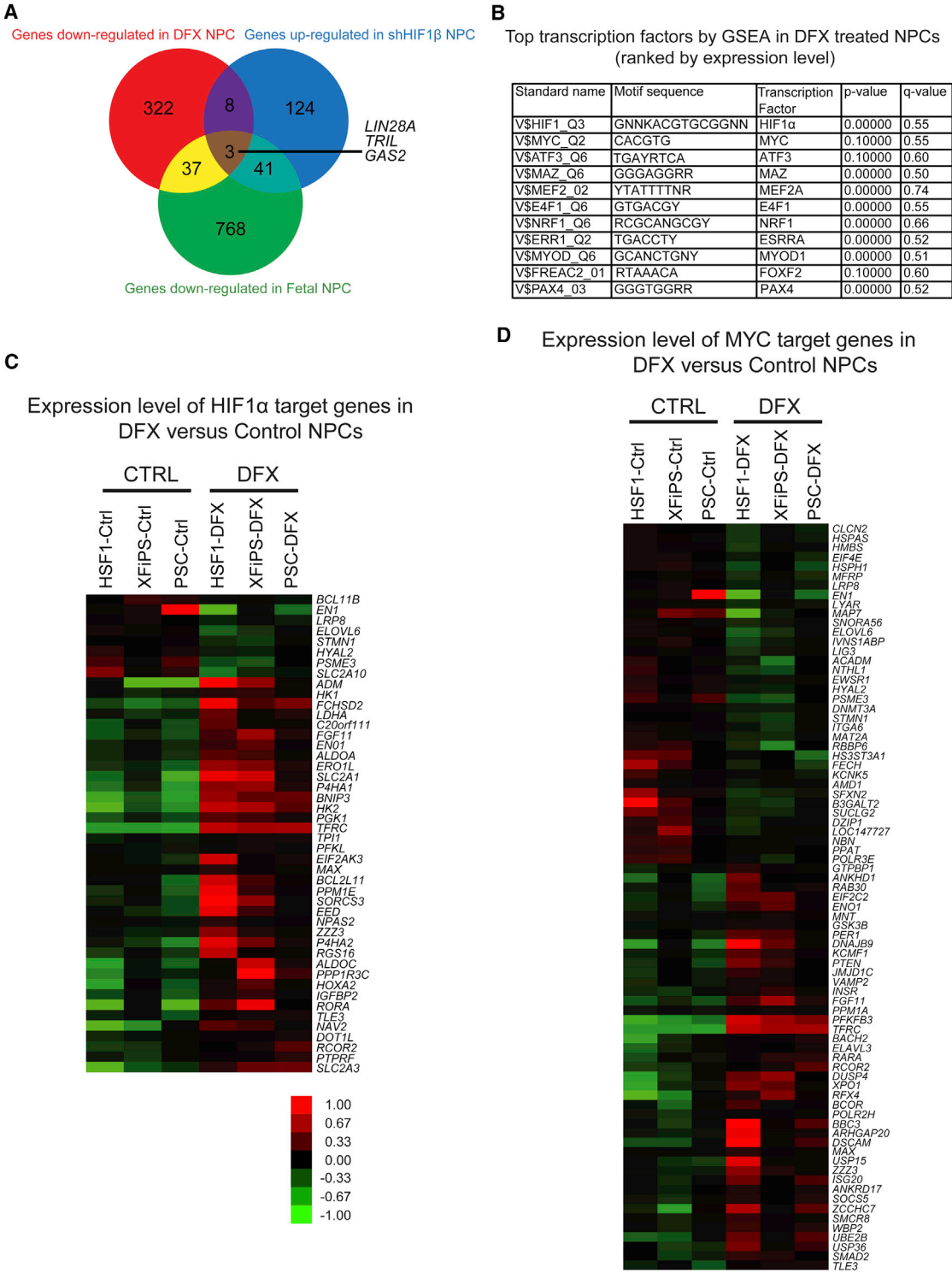
MYC stood out as an important regulator of HIF target genes because the binding sites for MYC and HIF can be highly overlapping (Figure 6A). One interesting gene that was affected by both HIF perturbation and known to be a MYC target gene is *LIN28*. The LIN28/*let-7* circuit can regulate developmental maturity in lower organisms, and the balance of activity of this circuit also correlates with neurogenic versus gliogenic potential in human NPCs (Patterson et al., 2012, 2014). The suppression of *LIN28* and gain of *let-7* miRNA expression is known to strongly correlate with the adoption of a gliogenic phenotype (La Torre et al., 2013; Patterson et al., 2012), as shown here by the induction of HIF activity. Based on these data, we explored the hypothesis that HIF regulates *LIN28* among a number of other target genes by competing for binding to specific gene promoters and displacing MYC.

To monitor transcriptional activity of the *LIN28* gene, we took advantage of an expression construct with defined MYC binding sites known to report transactivation of *LIN28B* (Chang et al., 2009). *LIN28B* reporter activity was induced with MYC overexpression (Figure 6A) and strongly suppressed by stabilization of HIF by DFX in a dose-dependent manner, consistent with HIF activity suppressing *LIN28B* expression (Figure 6B). Furthermore, when the MYC/HIF binding site within the *LIN28B* promoter was mutated, the reporter was no longer sensitive to DFX treatment (Figure 6B). In addition, both 2% O_2 and DFX drove a decrease in *LIN28A* and *LIN28B* expression levels in NPCs as measured by RT-PCR and immunostaining (Figures 6C and 6D), and as a result, mature *let-7* microRNA levels also increased (Figure 6E). Finally, using a reporter to detect *let-7* activity (Iwasaki et al., 2009), physiological O_2 significantly enhanced the activity of this family of miRNAs (Figure 6F). To explore the potential functional link between LIN28/*let-7* and O_2 tension in gliogenesis, DFX was combined with disruption of *let-7* levels. The ability of DFX to stimulate gliogenesis was completely abrogated by inhibition of *let-7* by antagomirs (Figures 6G and S4).

These combined results predict that manipulation of MYC in NPCs would affect the balance of neurons and glia produced during NPC differentiation. Human PSC-derived NPCs show a high level of expression for MYC family members, particularly N-MYC, whereas tissue derived progenitors isolated from midgestation brain are highly gliogenic and express negligible MYC (Patterson et al., 2014). Therefore, *N-MYC* was silenced in NPCs by siRNA to determine whether it plays a functional role in developmental maturity in this context (Figure 7A). Silencing *N-MYC* in NPCs decreased the expression of *LIN28A*, *LIN28B*, and *HMGA2* (Figure 7A), which are the genes known to promote neurogenesis (Patterson et al., 2014; Sanosaka et al., 2008).

Recently, it was shown that a small molecule inhibitor of BRD4 called JQ1 blocks transcription of *MYC* (Delmore et al., 2011; Mertz et al., 2011). To determine whether this inhibitor could also suppress *MYC* and *LIN28* expression, NPCs were treated with JQ1, which strongly

A

Genes down-regulated in DFX NPC   Genes up-regulated in shHIF1β NPC

LIN28A
TRIL
GAS2

Genes down-regulated in Fetal NPC

B

Top transcription factors by GSEA in DFX treated NPCs
(ranked by expression level)

Standard name	Motif sequence	Transcription Factor	p-value	q-value
V$HIF1_Q3	GNNKACGTGCGGNN	HIF1α	0.00000	0.55
V$MYC_Q2	CACGTG	MYC	0.10000	0.55
V$ATF3_Q6	TGAYRTCA	ATF3	0.10000	0.60
V$MAZ_Q6	GGGAGGRR	MAZ	0.00000	0.50
V$MEF2_02	YTATTTNR	MEF2A	0.00000	0.74
V$E4F1_Q6	GTGACGY	E4F1	0.00000	0.55
V$NRF1_Q6	RCGCANGCGY	NRF1	0.00000	0.66
V$ERR1_Q2	TGACCTY	ESRRA	0.00000	0.52
V$MYOD_Q6	GCANCTGNY	MYOD1	0.00000	0.51
V$FREAC2_01	RTAAACA	FOXF2	0.10000	0.60
V$PAX4_03	GGGTGGRR	PAX4	0.00000	0.52

C

Expression level of HIF1α target genes in
DFX versus Control NPCs

D

Expression level of MYC target genes in
DFX versus Control NPCs

Figure 5. Identification of Important Target Genes of the HIF Pathway in Neurogenesis

(A) Gene expression profiling led to the identification of numerous expression changes in response to altered HIF activity. Overlapping these gene expression changes identified three genes in common.

(B) GSEA was performed for the list of expression changes observed upon DFX treatment to identify transcription factors (TFs) that could be driving these changes. The list was narrowed by retaining only the TFs that were expressed in NPCs under either condition. Shown are the

(legend continued on next page)

suppressed *N-MYC* expression, but had little effect on *MYC* expression (Figure 7B). In addition, JQ1 treatment of NPCs led to decreased *LIN28A*, *LIN28B*, *HMGA2*, and *HES5* transcription (Figure 7B). This effect was quantifiable at the protein level as well for LIN28A and LIN28B (Figures 7C and 7D). All of these transcripts have been implicated in neurogenesis (Patterson et al., 2014; Sanosaka et al., 2008), and this pattern is consistent with a model in which JQ1 inhibits *N-MYC* expression, leading to lower *LIN28* expression, higher *let-7* activity, and lower expression of *let-7* target genes, such as *HMGA2*. Importantly, siRNA against *N-MYC* increased gliogenesis (Figure 7E). Furthermore, growth factor withdrawal to induce the differentiation of NPCs treated with JQ1 also shows a profound increase in gliogenesis (Figure 7F). Coupled with results using DFX, these data also provide relatively simple methods to improve the generation of glial cells in vitro.

DISCUSSION

The ability to culture human PSCs in vitro has opened up significant avenues of biological exploration from development to cancer. As experimenters attempt to recapitulate tissue-like environments in in vitro systems, one important consideration is the concentration of cell-permeable gasses such as O_2, nitric oxide, and CO_2. Almost all culture systems do not control for O_2 concentration and therefore use atmospheric O_2 levels. The physiological range of O_2 concentrations in brain tissues is much lower than atmospheric O_2 levels (Silver and Erecińska, 1998), and most studies of undirected or lineage specific differentiation in vitro have not considered O_2. Significant effort has delineated a role for O_2 tension in maintaining PSCs, with the consensus that these cells "prefer" physiological O_2 concentrations as judged by their ability to self-renew and express pluripotency factors (Forristal et al., 2010; Lengner et al., 2010; Mohyeldin et al., 2010; Westfall et al., 2008; Yoshida et al., 2009). Less is understood about the role of O_2 tension during differentiation, with the early embryo thought to be in a particularly hypoxic environment due to low vascularity prior to implantation. Even after implantation, there is heterogeneity in oxygen levels within the brain. Coupling this with the notion that pluripotent derivatives most accurately reflect cells found at the earliest stages of development, one could hypothe-size that pluripotent differentiation should be performed under low oxygen conditions to more closely recapitulate the situation into which these cells are normally born.

Our data demonstrate that the concentration of oxygen has profound effects on both undirected and directed differentiation of human PSCs. Portions of the pathway described here are consistent with the previous work describing neurogenesis in murine cells through Hif1, Lin28, and Myc (Balzer et al., 2010; Mutoh et al., 2012; Nagao et al., 2008). Here, we were able to piece together the entire pathway by which changes in oxygen concentration lead to altered cell fate decisions by NPCs and have done so in a human model. The fact that this was done in the human system is important because the relatively long time course typically required to generate glia in human PSC differentiation serves as a barrier to our understanding of nonneuronal cell types of the brain.

These findings provide a pathway by which neural progenitors can be driven through developmental stages to produce glia instead of neurons. At the most basic level, these data point toward relatively simple ways to guide developmental maturity of neural progenitors. More generally, these data could suggest that maintaining physiological oxygen concentrations could be important not only for more accurately recapitulating in vivo conditions, but also for preserving developmental timing during in vitro differentiation to yield cell types that are not born until later time points in utero.

The results presented here suggest that HIF and MYC are antagonistic to each other in neurogenesis. While others have suggested that this could be the case in other types of cells (Koshiji et al., 2004; Yoon et al., 2010), the mechanism proposed here is distinct. We found that a portion of MYC target sites in promoters also code for HIF binding. We propose a model whereby activation of HIF1α/β displaces MYC from targets such as LIN28, driving developmental progression. In our experiments, the use of low oxygen tension or hypoxia mimetics appeared to speed the process of development without dramatically altering the functional capacity of the cells generated.

An interesting aspect of these results is the fact that brief exposure to low oxygen or hypoxia mimetics was sufficient to induce the effect observed on developmental maturity. This suggests that low oxygen induces a lasting molecular change, perhaps in the epigenome of the cells. Significant effort will be required to identify such a change, but this

---

highest ranked TFs by both p value and expression level. Note that HIF and MYC were at the top of the list of TFs whose binding sites were enriched in genes that were changed by DFX.

(C) A heat map of established HIF target genes in DFX treated cells versus control. Red indicates induction; green indicates reduction.

(D) A heat map of established MYC target genes in DFX treated cells versus control.

See also Table S1.
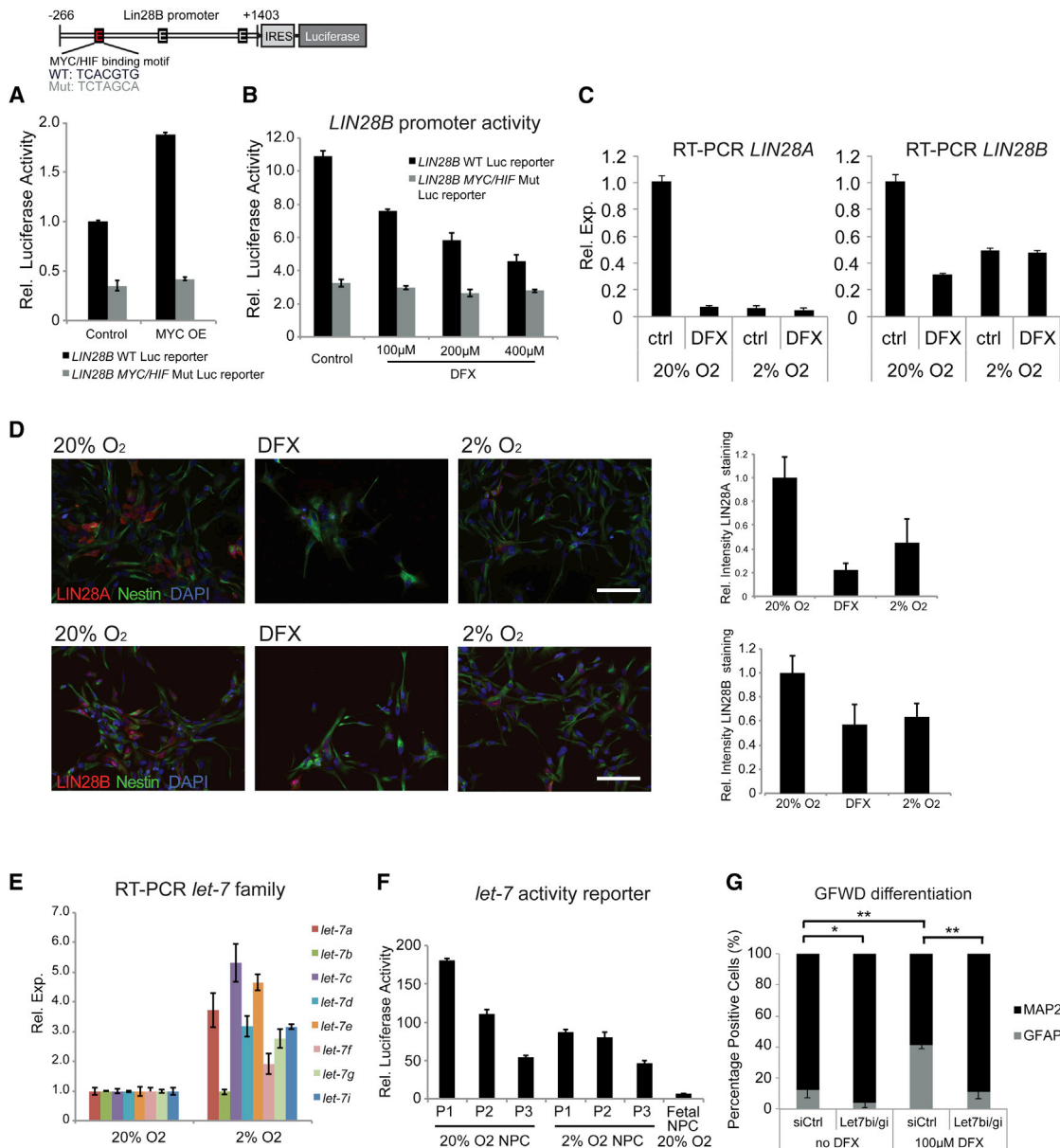
Figure 6. LIN28 Is Regulated Jointly by HIF and MYC through a Shared Binding Site

(A) A diagram shows the shared binding site of MYC and HIF in LIN28B promoter (MYC binding site "CACGTG," HIF binding site "TCACGT") (top). A luciferase-based promoter reporter for LIN28B showed a higher activity with overexpression of MYC, and a dramatic decrease in activity and insensitivity to MYC when the shared MYC/HIF binding site is mutated (bottom). Shown is relative luciferase activity normalized to constitutive reporter with and without activation by overexpression of MYC (n = 2 independent experiments; mean ± SD).

(B) The LIN28B reporter is suppressed by addition of DFX to the culture medium, and this effect is blocked in a reporter lacking a functional MYC/HIF site (n = 3 independent experiments; mean ± SD).

(C) Both *LIN28A* and *LIN28B* RNA expression were abrogated by either DFX treatment or exposure to physiological oxygen concentration (n = 3 independent experiments; mean ± SEM).

(D) Immunostaining for LIN28A and LIN28B in the indicated conditions demonstrates downregulation of these proteins in physiological oxygen or with DFX treatment. The effect is quantified (right) by intensity of staining on per cell basis (n > 100 cells per treatment; mean ± SEM; scale bars, 100 μm).

(E) RT-PCR for *let-7* family members shows an increase in physiological oxygen in NPCs (n = 2 independent experiments; mean ± SEM).

(legend continued on next page)

could lead to important insights into differences observed between NPCs born in tissue versus those born in culture in atmospheric oxygen (Patterson et al., 2014).

EXPERIMENTAL PROCEDURES

Cell Culture

hESCs and human induced PSCs (hiPSCs) were cultured as described previously (Patterson et al., 2012) in accordance with UCLA Embryonic Stem Cell Research Oversight committee. Experiments were performed on at least two independent hESC lines and one hiPSC line as indicated in the text. Feeder-free PSCs were maintained with mTeSR1 (Stem Cell Technologies) and passaged mechanically using StemPro EZPassage Tool (Invitrogen). Neural rosette derivation, NPC purification, and further differentiation to neurons and glia were performed as described (Patterson et al., 2012). Briefly, rosettes were generated by growing PSCs for at least 7 days in Dulbecco's modified Eagle's medium (DMEM)/F12 with N2 and B27 supplements (Invitrogen), 20 ng/ml basic fibroblast growth factor (FGF) (R&D Systems), 1 μM retinoic acid (RA) (Sigma), and 1 μM Sonic Hedgehog Agonist (Calbiochem). Once rosettes were picked, they were then cultured in NPC medium containing DMEM/F12, N2 and B27, 20 ng/ml basic FGF, and 500 ng/ml epidermal growth factor (EGF) (GIBCO). DFX (Sigma) (100 to 200 μM) and JQ1 (TOCRIS) (250 to 500 nM) were added at the NPC stage for 4 to 6 days, and their concentrations were adjusted for each cell line individually. Neural differentiation (growth factor withdrawal assay [GFWD]) was induced by withdrawing growth factors (EGF and FGF) from NPC medium for 2–6 weeks. Physiological oxygen tension growth was established in 2% O_2, 5% CO_2, and 92% N_2. Atmospheric oxygen tension growth was established in 20% O_2, 5% CO_2, and 75% N_2.

Immunofluorescent Staining and Quantification

Immunofluorescent staining was performed as described (Patterson et al., 2012). Antibodies used include the following: rabbit anti-TUJ1 (Covance, RPB-435P-100), chicken anti-GFAP (Abcam, ab4674), mouse anti-MAP2 (Abcam, ab11267), mouse anti-NESTIN (Neuromics, MO15012), rabbit anti-HIF1α (Novus, NB100-479), rabbit anti-LIN28A (Cell Signaling, A177), rabbit anti-LIN28B (Cell Signaling 4196S), and rabbit anticleaved caspase 3 (Cell Signaling, 9661). For the GFWD assay, cells grown on coverslips were fixed at different time points with 4% (w/v) paraformaldehyde (Electron Microscopy Sciences) in PBS. More than six views were randomly selected for each coverslip, and images were taken at 10× magnification with a consistent exposure time across all samples. Quantification was performed using ImageJ with the same threshold for each channel for all samples. The percentage of neurons and glia was calculated with positive staining area

that above the threshold of each channel and then scaled the total area of the neurons and glia to 100%. The percentage of neurons and glia from each experiment was then pooled to generate the figures, and the p value was calculated with Student's t test. The quantification based on cell number (DAPI staining) yielded similar results as those quantified by percentage (Figures S2B and S4). For the quantification of LIN28A and LIN28B, images were taken at 20× magnification with the consistent exposure time across all samples. Relative intensity was calculated by the ratio of the positive areas of LIN28A/B to the positive areas of total NPCs (measured by NESTIN). The same threshold for each channel was used across all samples. Relative intensity of nuclear HIF1α was quantified by the ratio of HIF1α-positive region within DAPI-positive region of each cell to the total DAPI area. Statistical analysis was done using a two-tailed, unpaired, Student's t test. Further details for each analysis are included in the figure legends accordingly.

EB Formation

EBs were generated as described (Chan et al., 2012). Briefly, embryonic stem cell colonies were dissociated from the plate mechanically using StemPro EZPassage Tool and cultured in ultralow attachment plates (Corning) containing DMEM/F12 supplemented with 20% knockout serum replacement medium (Invitrogen), L-glutamine (GIBCO), nonessential amino acids (GIBCO), and penicillin-streptomycin.

Generation of HIF-Deficient ESC Line

HIF1β, *HIF1α*, *HIF2α*, or scramble control shRNA *pLKO* lentiviral vector were purchased from Sigma. Lentivirus-infected hESCs or hiPSCs were selected by puromycin, as described before (Sherman et al., 2010).

Luciferase Reporter Assay

A *LIN28B* promoter driven luciferase reporter was kindly provided by Dr. Joshua T. Mendell (Johns Hopkins University School of Medicine) (Chang et al., 2009). Mutations in a *HIF/MYC* binding site were generated with a QuikChange II XL Site-Directed Mutagenesis Kit (Stratagene) and validated by sequencing. The mutant or the WT *LIN28B* promoter reporter was cotransfected with control or *c-MYC* plasmid (Addgene #13375) using lipofectamine 2000 (Life Technologies). Cells were lysed 48 hr after transfection and subjected to a Dual-Glo luciferase assay as described by the manufacturer (Promega). In DFX experiments, NPCs were transfected with the mutant or the WT *LIN28B* promoter luciferase reporter and then treated with DFX for 24 hr before lysed for a Dual-Glo luciferase assay. For *let-7* luciferase assay, NPCs cultured in 20% or 2% O_2 were transfected with the *psiCHECK2-let7* luciferase reporter (Addgene #20932) (Iwasaki et al., 2009) or the *psiCHECK2* control reporter (Promega), lysed 72 hr after

(F) A luciferase reporter with *let-7* binding sites in the 3′ UTR shows increased *let-7* activity (represented as decreased luciferase activity) in physiological oxygen, or over passage, which is known to induce *let-7* activity in PSC-NPCs. Fetal tissue derived NPC is known to have high *let-7* activity and serves as a positive control (Patterson et al., 2012) (n = 4 biological replicates; mean ± SD).

(G) The effect of DFX on gliogenesis is completely blocked by coordinated inhibition of *let-7* activity by the addition of *let-7* antagomirs (n = 3 independent experiments; mean ± SEM; *p < 0.05, **p < 0.01; Student's t test).

See also Figure S4.
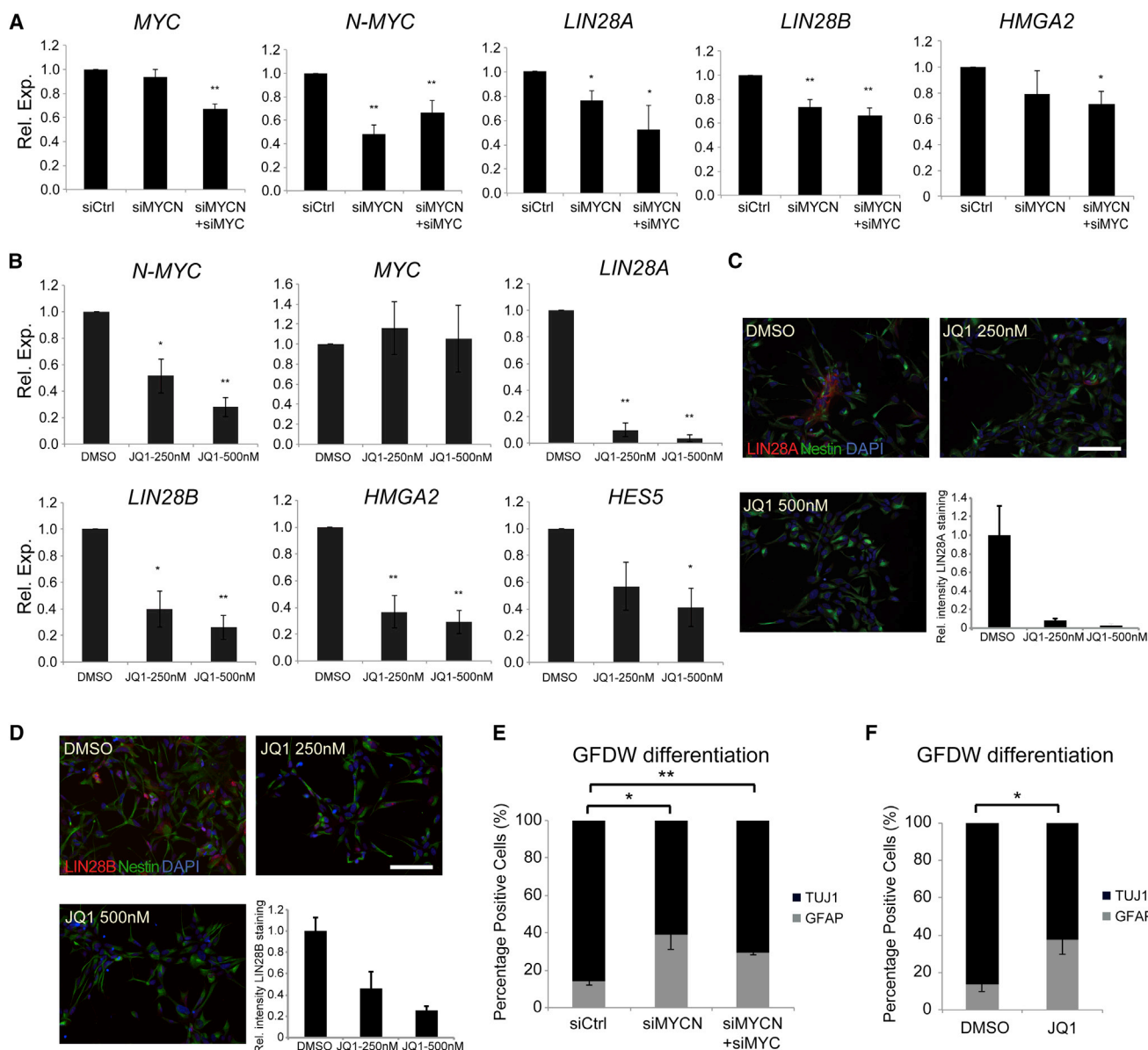
Figure 7. MYC Inhibition Mimics the Effect of HIF Activation to Suppress Immaturity Markers and Promote Gliogenesis

(A) Expression of *LIN28A*, *LIN28B*, and *HMGA2* after siRNA against *NMYC* and *MYC*. Values shown are relative to housekeeping gene (*beta actin*) (n = 3 independent experiments; mean ± SEM; *p < 0.05, **p < 0.01; Student's t test compared with interfering RNA against scrambled sequence [siCtrl]).

(B) PSC-NPCs were treated with two doses of JQ1, a small molecule inhibitor of *MYC* expression. NPCs treated with JQ1 showed decreased expression of *NMYC, LIN28A, LIN28B*, *HMGA2*, and *HES5* by RT-PCR (n = 3 independent experiments; mean ± SEM; *p < 0.05, **p < 0.01 compared with DMSO control; Student's t test).

(C and D) Expression of LIN28A and LIN28B proteins were measured by immunostaining and quantified on per cell basis (n > 600 cells for each treatment; mean ± SEM; scale bars, 100 μm).

(E and F) After knockdown of NMYC by siRNA, a GFWD assay shows increased gliogenesis from PSC-NPCs. (F) Treatment of PSC-NPCs with 250 nM JQ1 led to increased gliogenesis as measured by quantification of GFWD assay. (E and F, n = 4 independent experiments with either hESC or hiPSC-derived NPCs; mean ± SEM; *p < 0.05, **p < 0.01; Student's t test).

transfection, and subjected to a Dual-Glo luciferase assay. Luciferase assays were carried out in a GloMax 96 microplate luminometer (Promega).

let-7 Antagomir and siRNA Transfection
For the let-7 antagomir experiment, NPCs were treated with or without 100 μM DFX for 5 days before transfection. Cells was

then transfected with Dharmacon miRIDIAN human *let-7b* and *let-7g* hairpin inhibitor (Thermo Scientific) at a final concentration of 20 nM each or 40 nM miRIDIAN microRNA Hairpin Inhibitor Negative Control #1 (Thermo Scientific) using Lipofectamine RNAiMAX transfection reagent (Life Technologies) in accordance with the manufacturer's instructions. In the knockdown experiments, NPCs were transfected with unique 27-mer siRNA duplexes against human $HIF2\alpha$, $HIF1\beta$, *MYC*, and *MYCN* genes and the control duplex (Trilencer, Origene) at a final concentration of 40 nM (for double knockdown group, the final concentration is 20 nM of each siRNA) using Lipofectamine RNAiMAX transfection reagent. After transfection, cells were cultured in NPC medium for 5 days before growth factor withdrawal.

Gene Expression Analysis

RNA isolation, reverse transcription, and real-time PCR were performed as described (Lowry et al., 2008; Patterson et al., 2012). Total RNA was extracted using an RNeasy Mini Kit or a miRNeasy mini Kit (QIAGEN). cDNA was synthesized using the Superscript III first-strand cDNA synthesis kit (Invitrogen). Real-time PCR was performed using the SYBR green real-time PCR kit (Roche). Primer sequences are available upon request. In real-time PCR experiments, transcript levels were determined in triplicate reactions and normalized to a beta actin control. Mature *let-7* microRNAs were measured with miScript Primer Assays, miScript Reverse Transcription Kit, and miScript SYBR Green PCR kit (QIAGEN) according to manufacturer's instruction and normalized with the small RNA U6 as an internal control.

Microarray Profiling

Microarray profiling was performed with Affymetrix Human HG-U133 2.0 Plus arrays as described (Lowry et al., 2008). Data were normalized using the Robust Multichip Algorithm in Genespring (Agilent Technology). Probe sets expressed at a raw value of less than 50 in all samples were eliminated from further analysis. Gene expression differences were judged to be significant when a Student's t test p value was smaller than 0.05 and the fold change compared with a control was at least 1.54. GSEA was performed using the same criteria. Heat maps were generated using normalized expression data from the GSEA motif list, clustered using Cluster 3.0 software, and rendered by Java TreeView.

ACCESSION NUMBERS

Data were deposited in NIH Gene Expression Omnibus (GSE61842).

SUPPLEMENTAL INFORMATION

Supplemental Information includes Supplemental Experimental Procedures, four figures, and one table and can be found with this article online at http://dx.doi.org/10.1016/j.stemcr.2014.09.021.

AUTHOR CONTRIBUTIONS

Y.X. and J.Z. provided conception and design, collection and assembly of data, data analysis and interpretation, manuscript

REFERENCES

Adelman, D.M., Gertsenstein, M., Nagy, A., Simon, M.C., and Maltepe, E. (2000). Placental cell fates are regulated in vivo by HIF-mediated hypoxia responses. Genes Dev. *14*, 3191–3203.

Amarilio, R., Viukov, S.V., Sharir, A., Eshkar-Oren, I., Johnson, R.S., and Zelzer, E. (2007). HIF1alpha regulation of Sox9 is necessary to maintain differentiation of hypoxic prechondrogenic cells during early skeletogenesis. Development *134*, 3917–3928.

Balzer, E., Heine, C., Jiang, Q., Lee, V.M., and Moss, E.G. (2010). LIN28 alters cell fate succession and acts independently of the let-7 microRNA during neurogliogenesis in vitro. Development *137*, 891–900.

Chan, D.N., Azghadi, S.F., Feng, J., and Lowry, W.E. (2012). PTK7 marks the first human developmental EMT in vitro. PLoS ONE *7*, e50432.

Chang, T.C., Zeitels, L.R., Hwang, H.W., Chivukula, R.R., Wentzel, E.A., Dews, M., Jung, J., Gao, P., Dang, C.V., Beer, M.A., et al. (2009). Lin-28B transactivation is necessary for Myc-mediated let-7 repression and proliferation. Proc. Natl. Acad. Sci. USA *106*, 3384–3389.

Cimadamore, F., Amador-Arjona, A., Chen, C., Huang, C.T., and Terskikh, A.V. (2013). SOX2-LIN28/let-7 pathway regulates proliferation and neurogenesis in neural precursors. Proc. Natl. Acad. Sci. USA *110*, E3017–E3026.

Corn, P.G., Ricci, M.S., Scata, K.A., Arsham, A.M., Simon, M.C., Dicker, D.T., and El-Deiry, W.S. (2005). Mxi1 is induced by hypoxia in a HIF-1-dependent manner and protects cells from c-Myc-induced apoptosis. Cancer Biol. Ther. *4*, 1285–1294.

Covello, K.L., Kehler, J., Yu, H., Gordan, J.D., Arsham, A.M., Hu, C.J., Labosky, P.A., Simon, M.C., and Keith, B. (2006). HIF-2alpha regulates Oct-4: effects of hypoxia on stem cell function, embryonic development, and tumor growth. Genes Dev. *20*, 557–570.

Cowden Dahl, K.D., Fryer, B.H., Mack, F.A., Compernolle, V., Maltepe, E., Adelman, D.M., Carmeliet, P., and Simon, M.C. (2005). Hypoxia-inducible factors 1alpha and 2alpha regulate trophoblast differentiation. Mol. Cell. Biol. *25*, 10479–10491.

Delmore, J.E., Issa, G.C., Lemieux, M.E., Rahl, P.B., Shi, J., Jacobs, H.M., Kastritis, E., Gilpatrick, T., Paranal, R.M., Qi, J., et al. (2011). BET bromodomain inhibition as a therapeutic strategy to target c-Myc. Cell *146*, 904–917.

Denko, N.C. (2008). Hypoxia, HIF1 and glucose metabolism in the solid tumour. Nat. Rev. Cancer *8*, 705–713.

Dunwoodie, S.L. (2009). The role of hypoxia in development of the Mammalian embryo. Dev. Cell *17*, 755–773.

Ezashi, T., Das, P., and Roberts, R.M. (2005). Low O2 tensions and the prevention of differentiation of hES cells. Proc. Natl. Acad. Sci. USA *102*, 4783–4788.

Forristal, C.E., Wright, K.L., Hanley, N.A., Oreffo, R.O., and Houghton, F.D. (2010). Hypoxia inducible factors regulate pluripotency and proliferation in human embryonic stem cells cultured at reduced oxygen tensions. Reproduction *139*, 85–97.

Gordan, J.D., Bertout, J.A., Hu, C.J., Diehl, J.A., and Simon, M.C. (2007). HIF-2alpha promotes hypoxic cell proliferation by enhancing c-myc transcriptional activity. Cancer Cell *11*, 335–347.

Iwasaki, S., Kawamata, T., and Tomari, Y. (2009). Drosophila argonaute1 and argonaute2 employ distinct mechanisms for translational repression. Mol. Cell *34*, 58–67.

Kawahara, H., Okada, Y., Imai, T., Iwanami, A., Mischel, P.S., and Okano, H. (2011). Musashi1 cooperates in abnormal cell lineage protein 28 (Lin28)-mediated let-7 family microRNA biogenesis in early neural differentiation. J. Biol. Chem. *286*, 16121–16130.

Koshiji, M., Kageyama, Y., Pete, E.A., Horikawa, I., Barrett, J.C., and Huang, L.E. (2004). HIF-1alpha induces cell cycle arrest by functionally counteracting Myc. EMBO J. *23*, 1949–1956.

Kozak, K.R., Abbott, B., and Hankinson, O. (1997). ARNT-deficient mice and placental differentiation. Dev. Biol. *191*, 297–305.

Krishnan, J., Ahuja, P., Bodenmann, S., Knapik, D., Perriard, E., Krek, W., and Perriard, J.C. (2008). Essential role of developmentally activated hypoxia-inducible factor 1alpha for cardiac morphogenesis and function. Circ. Res. *103*, 1139–1146.

La Torre, A., Georgi, S., and Reh, T.A. (2013). Conserved microRNA pathway regulates developmental timing of retinal neurogenesis. Proc. Natl. Acad. Sci. USA *110*, E2362–E2370.

Lendahl, U., Lee, K.L., Yang, H., and Poellinger, L. (2009). Generating specificity and diversity in the transcriptional response to hypoxia. Nat. Rev. Genet. *10*, 821–832.

Lengner, C.J., Gimelbrant, A.A., Erwin, J.A., Cheng, A.W., Guenther, M.G., Welstead, G.G., Alagappan, R., Frampton, G.M., Xu, P., Muffat, J., et al. (2010). Derivation of pre-X inactivation human embryonic stem cells under physiological oxygen concentrations. Cell *141*, 872–883.

Licht, A.H., Müller-Holtkamp, F., Flamme, I., and Breier, G. (2006). Inhibition of hypoxia-inducible factor activity in endothelial cells disrupts embryonic cardiovascular development. Blood *107*, 584–590.

Lim, H.J., Han, J., Woo, D.H., Kim, S.E., Kim, S.K., Kang, H.G., and Kim, J.H. (2011). Biochemical and morphological effects of hypoxic environment on human embryonic stem cells in long-term culture and differentiating embryoid bodies. Mol. Cells *31*, 123–132.

Lowry, W.E., Richter, L., Yachechko, R., Pyle, A.D., Tchieu, J., Sridharan, R., Clark, A.T., and Plath, K. (2008). Generation of human induced pluripotent stem cells from dermal fibroblasts. Proc. Natl. Acad. Sci. USA *105*, 2883–2888.

Majmundar, A.J., Wong, W.J., and Simon, M.C. (2010). Hypoxia-inducible factors and the response to hypoxic stress. Mol. Cell *40*, 294–309.

Mertz, J.A., Conery, A.R., Bryant, B.M., Sandy, P., Balasubramanian, S., Mele, D.A., Bergeron, L., and Sims, R.J., 3rd. (2011). Targeting MYC dependence in cancer by inhibiting BET bromodomains. Proc. Natl. Acad. Sci. USA *108*, 16669–16674.

Miyata, T., Kawaguchi, D., Kawaguchi, A., and Gotoh, Y. (2010). Mechanisms that regulate the number of neurons during mouse neocortical development. Curr. Opin. Neurobiol. *20*, 22–28.

Mohyeldin, A., Garzón-Muvdi, T., and Quiñones-Hinojosa, A. (2010). Oxygen in stem cell biology: a critical component of the stem cell niche. Cell Stem Cell *7*, 150–161.

Mutoh, T., Sanosaka, T., Ito, K., and Nakashima, K. (2012). Oxygen levels epigenetically regulate fate switching of neural precursor cells via hypoxia-inducible factor 1α-notch signal interaction in the developing brain. Stem Cells *30*, 561–569.

Nagao, M., Campbell, K., Burns, K., Kuan, C.Y., Trumpp, A., and Nakafuku, M. (2008). Coordinated control of self-renewal and differentiation of neural stem cells by Myc and the p19ARF-p53 pathway. J. Cell Biol. *183*, 1243–1257.

Ng, K.M., Lee, Y.K., Chan, Y.C., Lai, W.H., Fung, M.L., Li, R.A., Siu, C.W., and Tse, H.F. (2010). Exogenous expression of HIF-1 alpha promotes cardiac differentiation of embryonic stem cells. J. Mol. Cell. Cardiol. *48*, 1129–1137.

Patterson, M., Chan, D.N., Ha, I., Case, D., Cui, Y., Van Handel, B., Mikkola, H.K., and Lowry, W.E. (2012). Defining the nature of human pluripotent stem cell progeny. Cell Res. *22*, 178–193.

Patterson, M., Gaeta, X., Loo, K., Edwards, M., Smale, S.T., Cinkornpumin, J., Xie, Y., Listgarten, J., Azghadi, S., Douglass, S., et al. (2014). let-7 miRNAs can act through notch to regulate human gliogenesis. Stem Cell Rep. Published online October 2, 2014. http://dx.doi.org/10.1016/j.stemcr.2014.08.015.

Prado-Lopez, S., Conesa, A., Armiñán, A., Martínez-Losa, M., Escobedo-Lucea, C., Gandia, C., Tarazona, S., Melguizo, D., Blesa, D., Montaner, D., et al. (2010). Hypoxia promotes efficient differentiation of human embryonic stem cells to functional endothelium. Stem Cells *28*, 407–418.

Provot, S., Zinyk, D., Gunes, Y., Kathri, R., Le, Q., Kronenberg, H.M., Johnson, R.S., Longaker, M.T., Giaccia, A.J., and Schipani, E. (2007). Hif-1alpha regulates differentiation of limb bud mesenchyme and joint development. J. Cell Biol. *177*, 451–464.

Sanosaka, T., Namihira, M., Asano, H., Kohyama, J., Aisaki, K., Igarashi, K., Kanno, J., and Nakashima, K. (2008). Identification of genes that restrict astrocyte differentiation of midgestational neural precursor cells. Neuroscience *155*, 780–788.

Sherman, M.H., Kuraishy, A.I., Deshpande, C., Hong, J.S., Cacalano, N.A., Gatti, R.A., Manis, J.P., Damore, M.A., Pellegrini, M., and Teitell, M.A. (2010). AID-induced genotoxic stress promotes B cell differentiation in the germinal center via ATM and LKB1 signaling. Mol. Cell *39*, 873–885.

Silver, I., and Erecińska, M. (1998). Oxygen and ion concentrations in normoxic and hypoxic brain cells. Adv. Exp. Med. Biol. *454*, 7–16.

Simon, M.C., and Keith, B. (2008). The role of oxygen availability in embryonic development and stem cell function. Nat. Rev. Mol. Cell Biol. *9*, 285–296.

Thomson, J.A., Itskovitz-Eldor, J., Shapiro, S.S., Waknitz, M.A., Swiergiel, J.J., Marshall, V.S., and Jones, J.M. (1998). Embryonic stem cell lines derived from human blastocysts. Science *282*, 1145–1147.

Tomita, S., Ueno, M., Sakamoto, M., Kitahama, Y., Ueki, M., Maekawa, N., Sakamoto, H., Gassmann, M., Kageyama, R., Ueda, N., et al. (2003). Defective brain development in mice lacking the Hif-1alpha gene in neural cells. Mol. Cell. Biol. *23*, 6739–6749.

Westfall, S.D., Sachdev, S., Das, P., Hearne, L.B., Hannink, M., Roberts, R.M., and Ezashi, T. (2008). Identification of oxygen-sensitive transcriptional programs in human embryonic stem cells. Stem Cells Dev. *17*, 869–881.

Wouters, B.G., and Koritzinsky, M. (2008). Hypoxia signalling through mTOR and the unfolded protein response in cancer. Nat. Rev. Cancer *8*, 851–864.

Xia, X., Lemieux, M.E., Li, W., Carroll, J.S., Brown, M., Liu, X.S., and Kung, A.L. (2009). Integrative analysis of HIF binding and transactivation reveals its role in maintaining histone methylation homeostasis. Proc. Natl. Acad. Sci. USA *106*, 4260–4265.

Yoon, D., Okhotin, D.V., Kim, B., Okhotina, Y., Okhotin, D.J., Miasnikova, G.Y., Sergueeva, A.I., Polyakova, L.A., Maslow, A., Lee, Y., et al. (2010). Increased size of solid organs in patients with Chuvash polycythemia and in mice with altered expression of HIF-1alpha and HIF-2alpha. J. Mol. Med. *88*, 523–530.

Yoshida, Y., Takahashi, K., Okita, K., Ichisaka, T., and Yamanaka, S. (2009). Hypoxia enhances the generation of induced pluripotent stem cells. Cell Stem Cell *5*, 237–241.

Zhang, H., Gao, P., Fukuda, R., Kumar, G., Krishnamachary, B., Zeller, K.I., Dang, C.V., and Semenza, G.L. (2007). HIF-1 inhibits mitochondrial biogenesis and cellular respiration in VHL-deficient renal cell carcinoma by repression of C-MYC activity. Cancer Cell *11*, 407–420.